A Study on Viscosity of Suspensions

WEN-YEN CHIU and TRONG-MING DON, *Department of Chemical Engineering, National Taiwan University, Taipei, Taiwan, Republic of China*

Synopsis

From a simple kinetic viewpoint for the formation and rupture of links among primary particles, the pseudoplastic behavior of suspensions can be well described. At steady state, the formation and rupture of links reach a dynamic equilibrium, and the viscosity of suspension is proportional to the state of aggregates. It is assumed that the formation of links is due to the surface forces over particles, including van der Waals' force, and is independent of shear rate. The rupture of links is proportional to $\dot{\gamma}^m$. Finally we get a very simple equation to predict the viscosity of suspension. With this simple kinetic viewpoint, the pseudoplastic behavior of suspensions composed of binary blends of monosize particles is also predictable.

INTRODUCTION

The rheological behavior of concentrated suspensions is the concern in this work. Those processes, such as pharmaceutical, food engineering, the production of solid rocket propellants and various filled polymeric materials, require understanding and control of rheological behavior of concentrated suspensions. Many factors, such as the shape, the size and size distribution of particles, temperature, particle concentrations, fluid field, the interaction, and aggregation of particles, may affect the viscosity of suspensions. Therefore, we must have a basic understanding on how these factors affect the viscosity of suspensions in casting, mixing, and transporting such materials.

Most of the theoretical efforts with suspensions have been directed toward the dilute limit, where the relative viscosity (η_r) of suspension is found to be independent of particle size and size distribution if electroviscous effects are absent. When particles are fully dispersed, the equations of the following form have been derived.[1,2]

$$\eta_r = 1 + k\phi + \cdots \tag{1}$$

where ϕ is the volume fraction of particles. Woods and Krieger[3] proposed eq. (2) to describe the shear stress dependent viscosity:

$$\eta_r = f(\phi, \tau_r) \tag{2}$$

by using dimensional analysis of the rheological and structural variables of monodispersed, uncharged, neutrally buoyant spheres. (τ_r is a dimensionless shear stress, $= \tau a^3/kT$, where τ is the shear stress, a is the particle radius, k Boltzmann constant, and T the absolute temperature.) Chong et al.[4] investigated the dependences of the viscosity of highly concentrated suspension on

Journal of Applied Polymer Science, Vol. 37, 2973–2986 (1989)
 CCC 0021-8995/89/102973-14$04.00

solid concentration and particle size distribution by using an orifice viscometer. They proposed an empirical equation [eq. (3)], to correlate the relative viscosity of suspension as a function of solid concentration and particle size distribution:

$$\eta_r = \left[1 + c\left(\frac{\phi/\phi_M}{1 - \phi/\phi_M}\right)\right]^2 \tag{3}$$

Here ϕ_M is the maximum packing factor, and $c = 0.75$. Fedors[5] also proposed a similar formula to correlate the relative viscosity with particle concentration, but the constant c is equal to 1.25.

Some theoretical analyses have been focused on the argument of structure kinetics of suspensions.[6-9] That the changes in rheological parameters are caused by the changes in the internal structure of suspensions. The nonlinear and time-dependent rheological behavior can be described by a set of two equations. The first, eq. (4), gives the instantaneous stress as a function of the instantaneous kinematics for every possible degree of structure, s. The second, eq. (5), is a kinetic equation which describes the rate of change of the degree of structure as a function of the instantaneous value of s and the instantaneous kinematics:

$$\tilde{\tau}(t) = f\left[\tilde{\dot{\gamma}}(t), s(t)\right] \tag{4}$$

$$\frac{ds(t)}{dt} = g\left[\tilde{\dot{\gamma}}(t), s(t)\right] \tag{5}$$

In this work, we adopt this kinetic view point to describe the pseudoplastic behavior of concentrated suspensions.

THEORETICAL CONSIDERATION

Viscosity of Suspension with Monosize Particles

If the flow of suspension shows a pseudoplastic behavior, it is that the suspended particles have interactions with each other and may aggregate in the suspension. To apply a flow field to the system, the number of particles in the aggregates or links among particles will be reduced by shearing force. That is why the viscosity of suspension changes as the shear rate changes. At transient state, the internal structure of suspension changes with time, because that the formation and rupture of aggregates occur simultaneously and do not reach an equilibrium state yet.

We assume the rupture of aggregates is proportional to the $\dot{\gamma}^m$, i.e.,

$$\frac{dn_l}{dt} = k_l n i^m \tag{6}$$

where $\dot{\gamma}$ is shear rate, m is a parameter, dn_l/dt is the loss rate of particles per aggregate, n is the current structural state, and k_l is the loss rate constant. The growth of aggregate is due to the surface forces among particles (includ-

ing van der Waals' force), and is assumed to be independent of shear rate as expressed in

$$\frac{dn_c}{dt} = \frac{k_c}{\lambda^m}(n_0 - n) \tag{7}$$

where dn_c/dt is the growth rate of a typical aggregate, n_0 is the saturated structural state, a situation achieved at equilibrium when $\dot{r} = 0$ has prevailed sufficiently long, k_c is the growth rate constant, and λ is a characteristic time for growth of aggregates.

(i) At steady state, the two processes influencing the structural state of the fluid reach a balance. Equating eqs. (6) and (7) leads to the structural contribution to the shear rate dependent viscosity, $\eta_{agg}(\dot{r})$.

$$\frac{\eta_{agg}(\dot{r})}{\eta_{agg,0}} = \frac{n(\dot{r})}{n_0} = P(\dot{r}) = \frac{1}{1 + b\dot{r}^m} \tag{8}$$

Here we assume the viscosity induced by aggregation is proportional to the structural state. $\eta_{agg}(\dot{r})$ and $\eta_{agg,0}$ are viscosities due to aggregation under shear rate $\dot{r}$ and saturated equilibrium ($\dot{r} = 0$). $P(\dot{r})$ is the structure parameter under shear rate $\dot{r}$ and $b = (k_l/k_c)\lambda^m$. The total viscosity must include an additional frictional resistance experienced when the particles are all dispersed under very high shear rate. So

$$\eta(\dot{r}) = \eta_{agg}(\dot{r}) + \eta_\infty$$

Upon rearrangement,

$$\frac{\eta(\dot{r}) - \eta_\infty}{\eta_0 - \eta_\infty} = \frac{1}{1 + b\dot{r}^m} \tag{9}$$

Here η_∞ is the infinite shear rate viscosity, and η_0 is the zero-shear-rate viscosity. Let $\beta = \eta_\infty/\eta_0$; eq. (9) can be cast into dimensionless form:

$$\frac{\eta(\dot{r})}{\eta_0} = \frac{1 - \beta}{1 + b\dot{r}^m} + \beta \tag{10}$$

From the calculation of eq. (10), the relationship between viscosity of suspension and shear rate can be predicted.

(ii) At unsteady state:

(a) A step function in shear rate, that is,

$$\text{at } t = 0, \quad \dot{r} = 0, \quad \text{and} \quad \text{at } t \geq 0^+, \quad \dot{r} = \dot{r}_0 = \text{const}$$

From eqs. (6) and (7), the structure parameter, $P(t) = \eta(t)/\eta_0$, can be derived as

$$\frac{dP(t)}{dt} = \frac{k_c}{\lambda^m}(1 - P) - k_l P\dot{r}^m \tag{11}$$

with $\dot{r} = \dot{r}_0$ and the initial condition $P(0) = 1$. From eq. (11), we solve $P(t)$ as

$$P(t) = P_{ss}(\dot{r}_0) + [1 - P_{ss}(\dot{r}_0)] \times \exp[-k_l t/bP_{ss}(\dot{r}_0)] \tag{12}$$

where $P_{ss}(\dot{r}_0) = 1/1 + b\dot{r}_0^m$ is the steady value under constant shear rate $\dot{r}_0$.

(b) Stress relaxation: First the sample is sheared homogeneously ($\dot{r} = \dot{r}_0$) until it reaches the steady state. Then a sudden release in shear rate follows; i.e., $\dot{r} = \dot{r}_0$ at $t \leq 0^-$, and $\dot{r} = 0$ at $t \geq 0^+$. From eq. (11) with $\dot{r} = 0$ and the initial condition $P(0) = P_{ss}(\dot{r}_0)$, we solve $P(t)$ as

$$P(t) = 1 + [P_{ss}(\dot{r}_0) - 1]\exp(-k_l t/b) \tag{13}$$

(c) A linear increase in shear rate, $\dot{r} = at$, and a is a constant value. Then from eq. (11) with $\dot{r} = at$ and the initial condition $P(0) = 1$, we solve $P(t)$ as

$$P(t) = \frac{\left[1 + \frac{k_l}{b}\int_0^t \exp\left(\frac{k_l}{b}t + \frac{k_l a^m}{m+1}t^{m+1}\right) dt\right]}{\left[\exp\left(\frac{k_l}{b}t + \frac{k_l a^m}{m+1}t^{m+1}\right)\right]} \tag{14}$$

In all these three situations above, the corresponding unsteady viscosity of suspension can be predicted by

$$\frac{\eta(t) - \eta_\infty}{\eta_0 - \eta_\infty} = P(t) \tag{15}$$

Therefore, the values of η_0, η_∞, b, and m can be determined from steady state experiments and curve fitting of eq. (10). And two more values, k_l and k_c/λ^m, can be determined through any unsteady state experiments and curve fitting of eq. (15).

Viscosity of Suspension Composed of Binary Sizes of Particles

Introducing the composition dependent coefficient (ϕ) [10] to the mixing rule in order to describe the intercomponent interactions of two different sizes of particles:

$$\eta_{b,\,\mathrm{agg}} = \phi_s \omega_s \eta_{s,\,\mathrm{agg}} + \phi_L \omega_L \eta_{L,\,\mathrm{agg}} \tag{16}$$

where ϕ_s and ϕ_L are the coefficients for small particles and large particles, respectively, ω_s and ω_L are weight fractions of small and large particles. The subscripts b, s, and L mean the situations in blending, pure small particles, and pure large particles. At very high shear rate, all the particles are dispersed

and the interactions among particles can be neglected, i.e.,

$$\eta_{b,\infty} = \omega_s \eta_{s,\infty} + \omega_L \eta_{L,\infty} \tag{17}$$

From eqs. (9), (16), and (17), we can get

$$\eta_b(\dot{r}) = \frac{\phi_s \omega_s (\eta_{s,0} - \eta_{s,\infty})}{1 + b_s \dot{r}^m} + \frac{\phi_L \omega_L (\eta_{L,0} - \eta_{L,\infty})}{1 + b_L \dot{r}^m}$$

$$+ \omega_s \eta_{s,\infty} + \omega_L \eta_{L,\infty} \tag{18}$$

The aggregation of particles is closely related to the surface area of particles. Considering the aggregation of one small particle and one large particle, the fraction of contact area between two to the surface area of the small particle is much larger than that of the large particle. In other words, the aggregation for small particle is significantly affected by large particle, but the effect of small particle to large particle is minor. Therefore, we assume that the characteristic time of small particles for aggregation in the blending state is affected by the large particles, but the characteristic time of large particles remains unaffected. That is,

$$\lambda_s(w) = \phi_s(w)\lambda_s^0 = w_s \lambda_s^0 + w_L \lambda_L^0 \tag{19}$$

$$\lambda_L(w) = \phi_L(w)\lambda_L^0 = \lambda_L^0 \tag{20}$$

where superscript 0 denotes component properties in the pure state. Equation (19) means that λ_s is calculated from two contributions, that corresponding to intracomponent interactions ($w_s \lambda_s^0$) and that corresponding to intercomponent interactions ($w_L \lambda_L^0$). Equation (20) reveals that λ_L of large particles is not affected by the presence of small particles.

From the above two equations, we get the composition-dependent coefficient ϕ as follows:

$$\phi_s(w) = \frac{w_L \lambda_L^0}{\lambda_s^0} + w_s \tag{21}$$

$$\phi_L(w) = 1 \tag{22}$$

Since the rate constants k_c and k_l are only dependent on temperature and the nature of particles. So eqs. (21) and (22) can be rewritten as

$$\phi_s(w) = w_L \left(b_L^0 / b_s^0 \right)^{1/m} + w_s \tag{23}$$

$$\phi_L(w) = 1 \tag{24}$$

With the help of eqs. (19) and (20), we can evaluate $b_s(w)$ and $b_L(w)$ by

$$b_s(w) = \frac{k_l}{k_c}\lambda_s^m = \frac{k_l}{k_c}\left(w_s\lambda_s^0 + w_L\lambda_L^0\right)^m$$

$$= \left(w_s b_s^{0\,1/m} + w_L b_L^{0\,1/m}\right)^m \tag{25}$$

$$b_L(w) = \frac{k_l}{k_c}\lambda_L^m = \frac{k_l}{k_c}\left(\lambda_L^0\right)^m = b_L^0 \tag{26}$$

Therefore, we can predict the viscosity of suspension composed of binary sizes of particles through eqs. (18), (23), (24), (25), and (26), as long as we know the viscosities of two pure suspensions with monosize particles.

EXPERIMENTAL

Sample Preparation

The suspension medium is HTPB (hydroxyl terminated polybutadiene, average molecular weight 2800, hydroxyl value 0.83 meq/g, *trans*-1,4 60%, *cis*-1,4 20%, and vinyl-1,2 20%) supplied by Arco. Co., Ltd. Before the test of viscosity, we demoisture the HTPB by vacuum heating in the oil bath at 90°C and 5 mm Hg. The #70 (diam 210–250 μm) and #325 (diam 44–53 μm) salt (NaCl) particles are selected as fillers in HTPB. The filler content is 60 wt % in all viscosity tests.

Viscosity Measurement

Steady viscosity and unsteady viscosity are all measured with a duplex cylinder rheometer at 35°C (see Fig. 1). From steady state experiments, the viscosity of suspension vs. shear rate relationship is observed. In unsteady state experiments, shear rate is set in a linear increase, i.e., $\dot{r} = at$. And the viscosity of suspension vs. time curve is obtained. From which the best k_l/b value can be determined through the curve fitting of experimental data with eq. (15). The parameter a is chosen as 3.168 or 2.112 in this work.

Determination of Maximum Packing Factor (ϕ_M)

For the determination of ϕ_M, a reference system (40 wt % NaCl in *n*-butanol) is used instead of 60 wt % NaCl in HTPB, because the lower viscosity of reference system makes it much easier to get ϕ_M value from both gravity method and centrifugal force method. Therefore, the ϕ_M values obtained from our experiments are only considered as a reference, which helps explain the discrepancy between experimental data and theoretical prediction of viscosity.

The testing suspension is kept in a long and thin tube at 35°C for some time by gravitation force or centrifugal force until the height of thick layer (containing NaCl particles) remains unchanged. Then the maximum packing

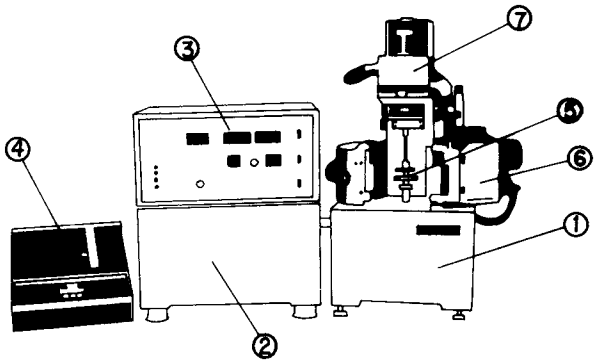

An outside view of Rheometer

1. Main measurment device
2. Driving portion
3. Operation portion
4. X - Y Recorder
5. Duplex cylinder (Outer cylinder Ø 22 mm, Inner cylinder Ø 18 mm)
6. Air bath
7. Detective portion

Fig. 1. An outside view of rheometer: (1) main measurement device; (2) driving portion; (3) operation portion; (4) X-Y recorder; (5) duplex cylinder (outer cylinder ϕ 22 mm, inner cylinder ϕ 18 mm); (6) air bath; (7) detective portion.

factor can be calculated through the following equation:

$$\phi_M = \frac{40/\varphi_s}{h_f/h_i(40/\varphi_s + 60/\varphi_e)} \tag{27}$$

where h_i = total height of suspension, h_f = height of thick layer, φ_e = density of n-butanol (= 0.805 g/cm^3 at 35°C), and φ_s = density of NaCl (= 2.17 g/cm^3).

RESULTS AND DISCUSSION

As in Figure 2, the viscosity of pure HTPB liquid keeps at a constant value, 46 P, at 35°C in the shear rate range of tests. Also we can find from the figure that, as the particle size is smaller, the increase in viscosity of suspension is more evident, especially at low shear rate, and the pseudoplastic behavior also is more significant. This phenomenon probably is related to the increase of surface area of particles per unit volume. Because the small particles have much more surface areas per unit volume, their interactions, hence aggregations of particles, are much stronger especially in low shear rate region.

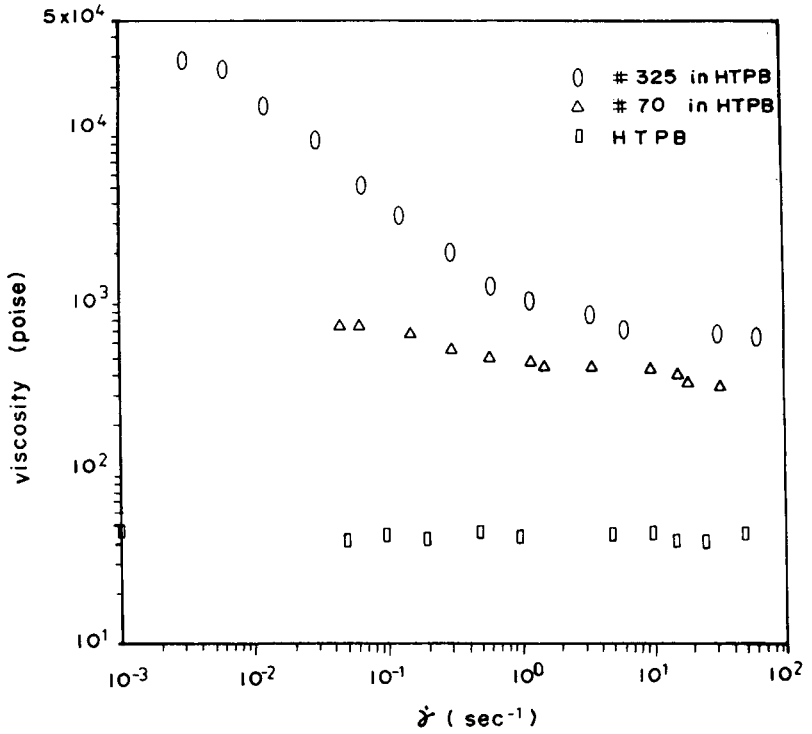

Fig. 2. Effect of particle size on viscosity of suspension at 35°C, particle concentration = 60 wt %: (○) #325 in HTPB; (△) #70 in HTPB; (□) HTPB.

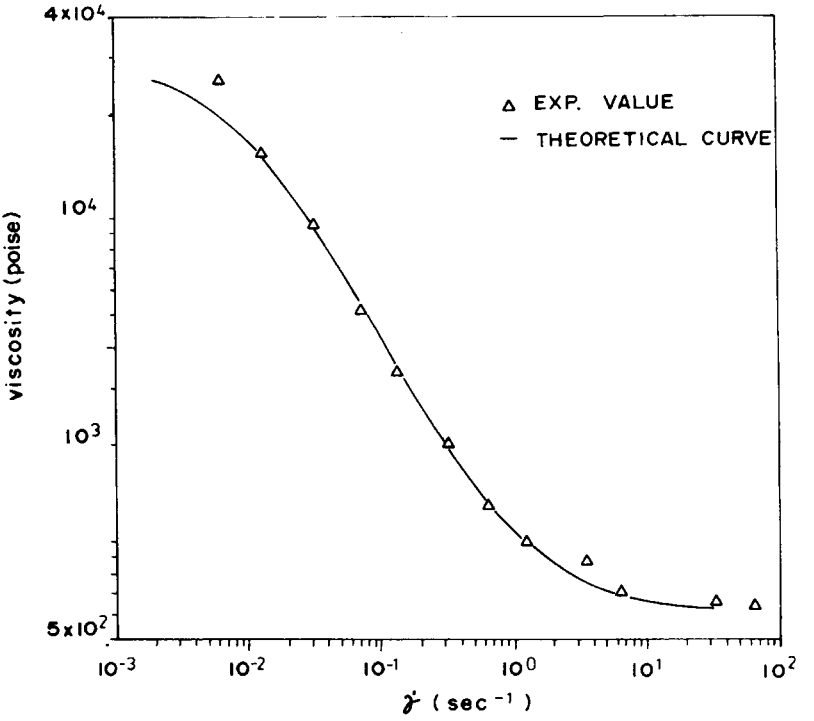

Fig. 3. Viscosity of suspension with #325 NaCl in HTPB vs. shear rate at 35°C, particle concentration = 60 wt %: (△) exptl value; (—) theoretical curve.

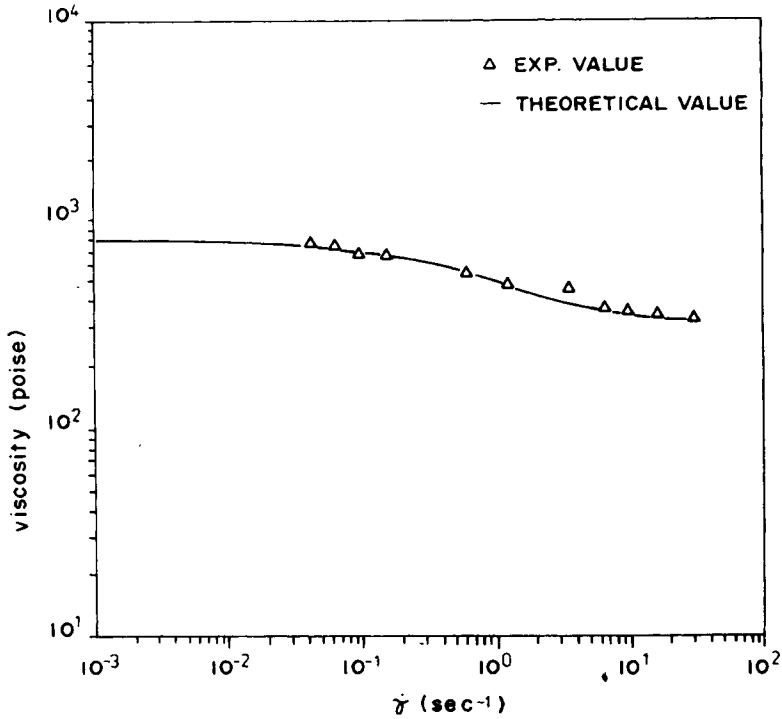

Fig. 4. Viscosity of suspension with #70 NaCl in HTPB vs. shear rate at 35°C, particle concentration = 60 wt %: (Δ) exptl value; (—) theoretical curve.

In Figures 3 and 4, we use the kinetic viewpoint, eq. (10), to describe the pseudoplastic behavior of suspensions filled with #325 and #70 NaCl, respectively. The experimental data are also shown in figures for comparison. The values of η_0, η_∞, m, and b are obtained as 3×10^4 (P), 600 (P), 0.934, and 58.93 for the suspension filled with #325 NaCl and those for suspension filled with #70 NaCl are 800 (P), 320 (P), 0.94, and 2.14 by curve fitting. Since the rate constants are only dependent on the nature of particles, the characteristic time of aggregation for #325 NaCl particles is then about 34 times of that for #70 particles $[(b_s/b_L)^{1/m} = \lambda_s/\lambda_L]$.

When the shear rate is in linear increase, we can find out the k_l/b value through eqs. (14) and (15) along with the experimental curve as shown in Figures 5 and 6. It is seen that the k_l/b value is in the range of 0.4–0.6 for small particles (#325) and 5–10 for large particles (#70). So the characteristic time calculated for #325 NaCl is about 10–30 times of that for #70 NaCl. This is close to the value found in Figures 3 and 4. From above discussion, we know that the characteristic time of aggregation is approximately proportional to the inverse of the surface area of particle.

The kinetic aggregation model [eqs. (18), (23)–(26)] can also be used to predict the pseudoplastic behavior of suspensions composed of two kinds of monosize particles as in Figures 7–11. It is found that the theoretical prediction is very close to the experimental data, except in the case of Figure 11 with 20 wt % small particles in total solid particles. The predicted viscosities of

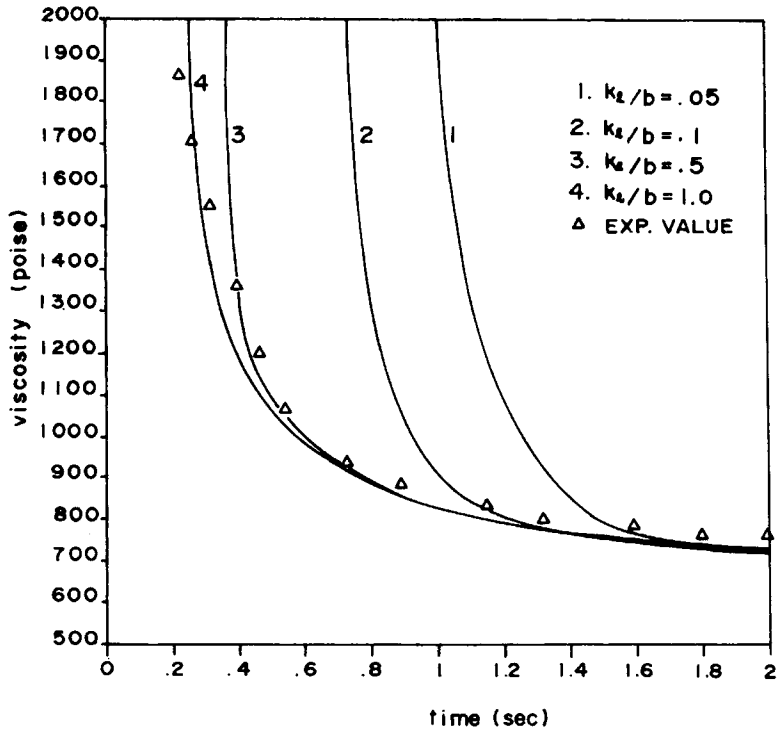

Fig. 5. Viscosity of suspension with #325 NaCl in HTPB vs. time at 35°C under unsteady state experiment, $\dot{r} = 3.168\ t$, particle concentration = 60 wt %. k_l/b: (1) 0.05; (2) 0.1; (3) 0.5; (4) 1.0; (△) exptl value.

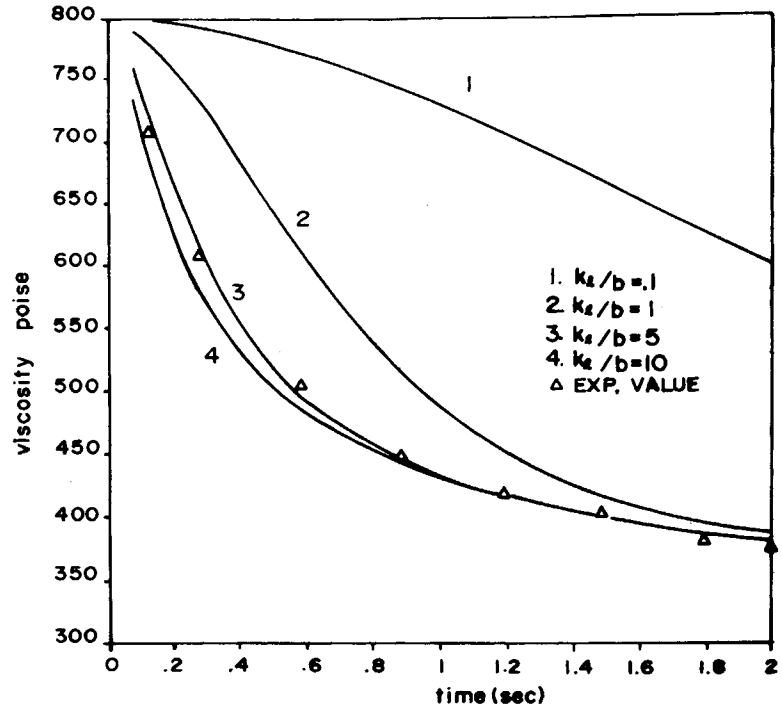

Fig. 6. Viscosity of suspension with #70 NaCl in HTPB vs. time at 35°C under unsteady state experiment, $\dot{r} = 2.112\ t$, particle concentration = 60 wt %. k_l/b: (1) 0.1; (2) 1; (3) 5; (4) 10; (△) exptl value.

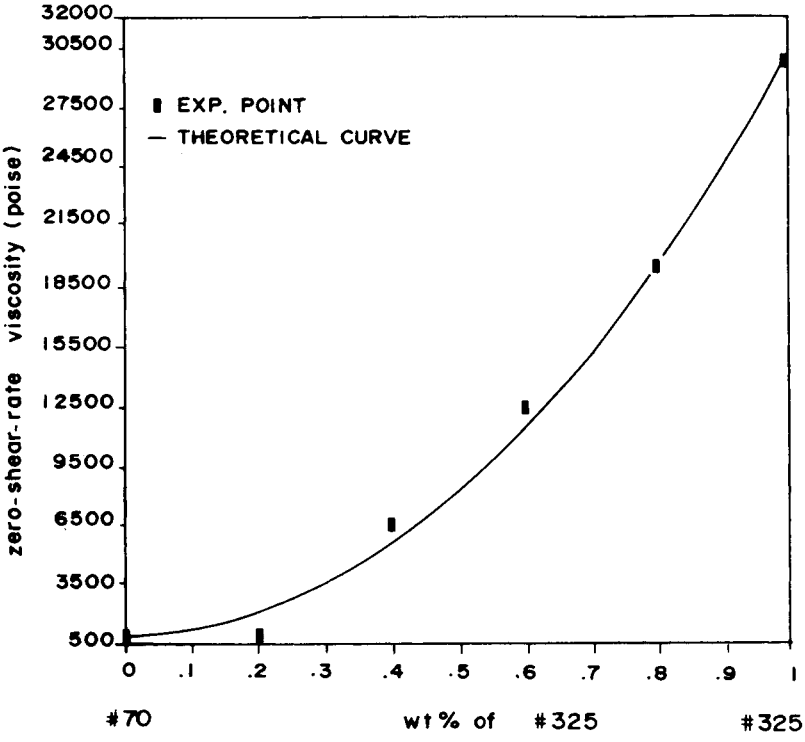

Fig. 7. Zero-shear-rate viscosity of suspension with binary blends of particle at 35°C, total particle concentration = 60 wt %: (■) exptl point; (—) theoretical curve.

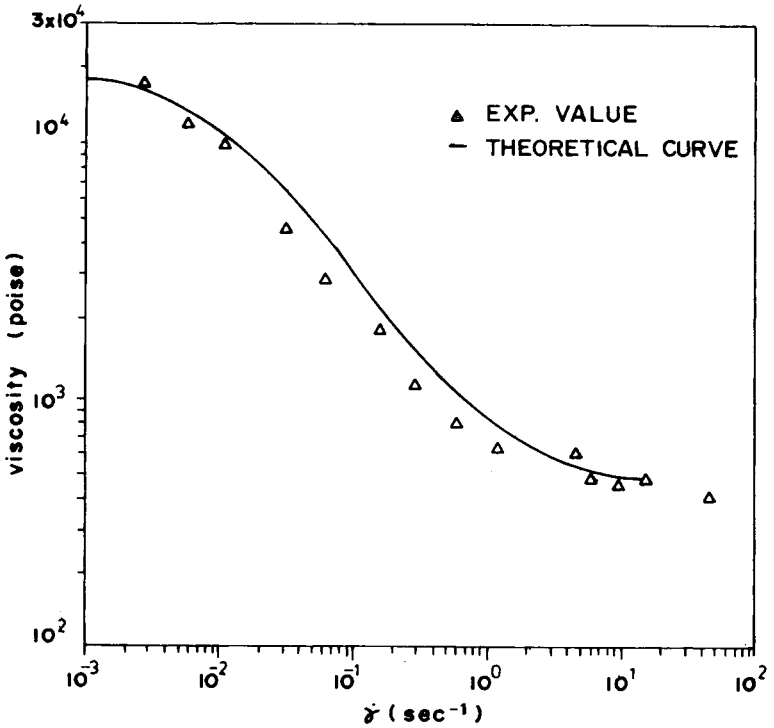

Fig. 8. Viscosity of suspension with binary blends of particles at 35°C, #325 NaCl/#70 NaCl = 8/2, total particle concentration = 60 wt %: (△) exptl value; (—) theoretical curve.

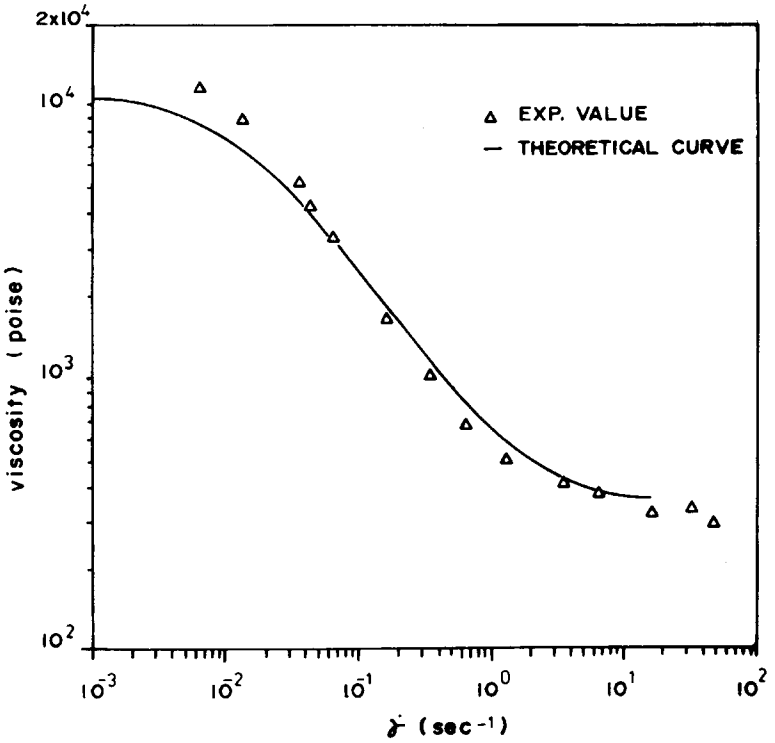

Fig. 9. Viscosity of suspension with binary blends of particles at 35°C, #325 NaCl/#70 NaCl = 6/4, total particle concentration = 60 wt %: (△) exptl value; (—) theoretical curve.

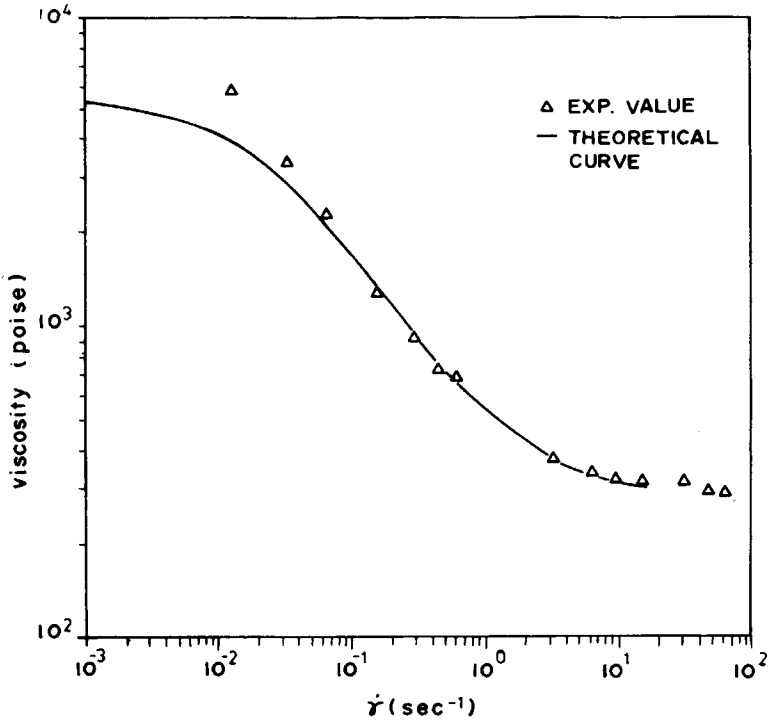

Fig. 10. Viscosity of suspension with binary blends of particles at 35°C, #325 NaCl/#70 NaCl = 4/6, total particle concentration = 60 wt %: (△) exptl value; (—) theoretical curve.

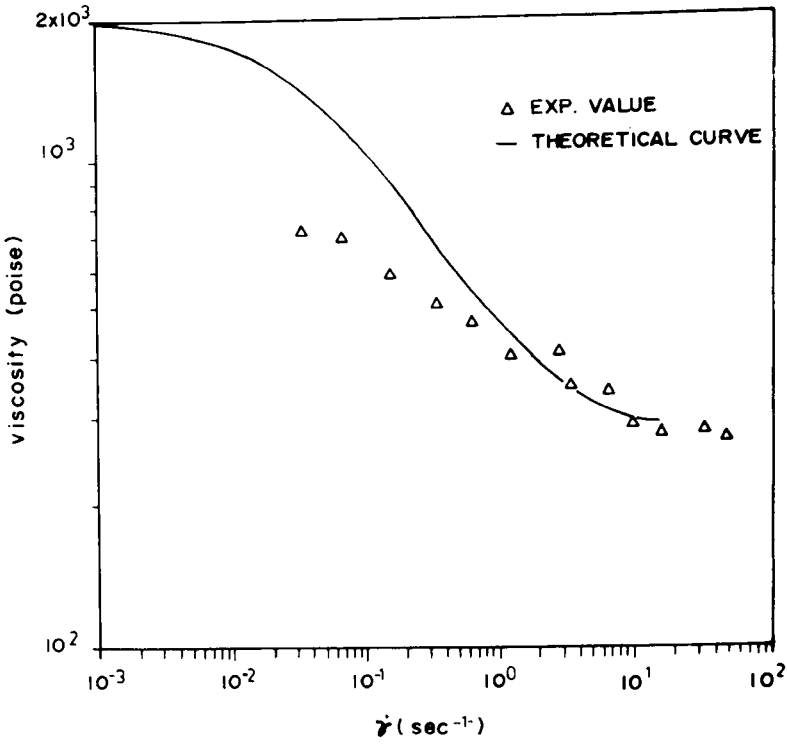

Fig. 11. Viscosity of suspension with binary blends of particles at 35°C, #325 NaCl/#70 NaCl = 2/8, total particle concentration = 60 wt %: (△) exptl value; (—) theoretical curve.

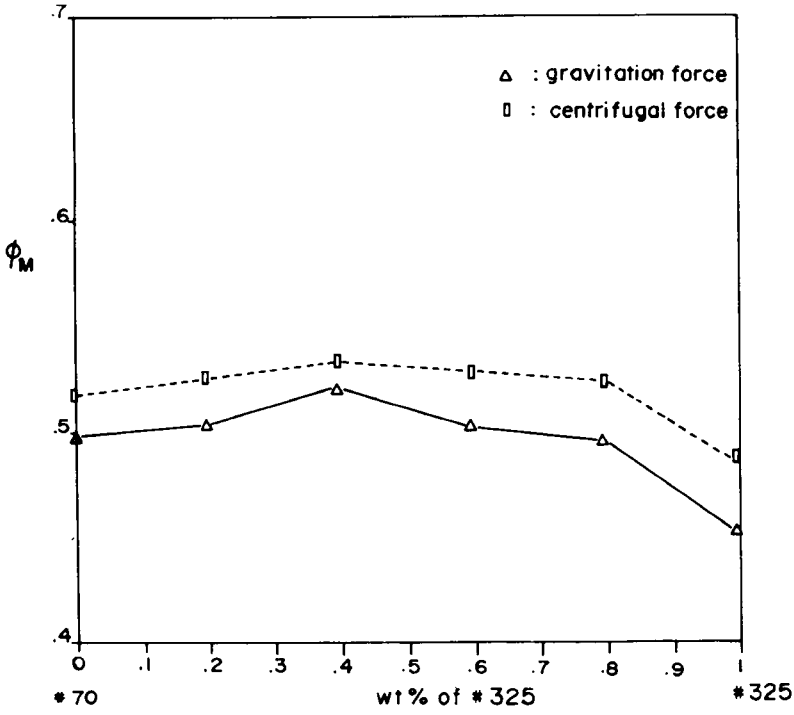

Fig. 12. Maximum packing factor versus size-composition of NaCl in *n*-butanol at 35°C, particle concentration = 40 wt %: (△) gravitational force; (▯) centrifugal force.

suspensions in Figure 11 are higher than the experimental ones in low shear rate region. Chong et al.[4] discussed the effect of particle size distribution on viscosity of suspension with glass beads dispersed in PIB liquid. They found that the minimum viscosity of a bimodal system could be achieved with 25–35% of solids as fine spheres, the remainder being the coarse size. This decrease in viscosity can be explained by the increase of the maximum packing factor (ϕ_M). Generally, ϕ_M is assumed to be 0.63 for dense random packing of large particle spheres of uniform size. But it can be smaller due to the effect of aggregation. On the other hand, polydispersity can make the ϕ_M value increase, since the small particles can fit in the vacancies between large particles. As the ϕ_M value increases, the relative viscosity then decreases through the relation of eq. (3). Figure 12 shows the ϕ_M values of NaCl in *n*-butanol suspensions obtained in our experiments, which are smaller than 0.63 due to the effect of aggregation. Also ϕ_M varies with the size–composition of solid particles, and can attain higher value in the middle range of weight fraction. But in our theoretical work, we did not consider the variation of ϕ_M in bimodal system. That might be the main cause for the discrepancy found in Figure 11.

References

1. C. R. Wildemuth and M. C. Williams, *Rheol. Acta*, **23**, 627 (1984).
2. John Happel and Howard Brenner, *Low Reynolds Number Hydrodynamics*, chapter 9. Prentice-Hall, Englewood Cliffs, NJ, 1965.
3. M. E. Woods and I. M. Krieger, *J. Colloid Interface Sci.*, **34**, 91 (1970).
4. J.-S. Chong, E. B. Christiansen, and A. D. Baer, *J. Appl. Polym. Sci.*, **15**, 2007 (1971).
5. R. F. Fedors, *J. Colloid Interface Sci.*, **46**, 545 (1974).
6. J. Mewis, *J. Non-Newt. Fluid Mech.*, **6**, 1 (1979).
7. M. M. Cross, *J. Colloid Sci.*, **20**, 417 (1965).
8. M. M. Cross, *J. Colloid Interface Sci.*, **33**, 30 (1970).
9. W. Y. Chiu, M. D. Hughes, and D. S. Soon, *Polym. Proc. Eng.*, **2**(1), 69 (1984).
10. Tony Y. Liu, D. S. Soong and M. C. Williams, *J. Rheol.*, **27**, 7 (1983).

Received March 15, 1988
Accepted May 12, 1988